Influence of defects on the critical behaviour at the 105 K structural phase transition of $SrTiO_3$: I. The broad component

H. Hünnefeld, T. Niemöller, and J. R. Schneider
Hamburger Synchrotronstrahlungslabor HASYLAB at Deutsches Elektronen-Synchrotron DESY, Notkestr. 85, D-22603 Hamburg, Germany

B. A. Kaufmann and F. Schwabl
Lehrstuhl für Theoretische Physik V, Physik-Department der Technischen Universität München, James-Franck-Straße, D-85747 Garching, Germany

(June 7, 2000)

The critical fluctuations in $SrTiO_3$ near its $105\,K$ structural phase transition were studied with triple axis diffractometry using high energy ($\geq 100\,keV$) synchrotron radiation in different $SrTiO_3$ crystals with different oxygen vacancy concentrations. Due to the presence of oxygen vacancies the critical behaviour is changed compared to defect-free systems. In our experiments a smearing out of the squared order parameter and a crossover of the critical exponents ν and γ above the phase transition temperature is observed, with the crossover temperature strongly depending on the concentration of the defects. To understand the experimental findings, e.g. the unusual values for the critical exponents found near the critical temperature, the Ginzburg-Landau-Wilson functional for structural phase transitions in disordered systems was analyzed using renormalization group theory and the replica trick. Considering the effects of defects which locally increase the transition temperature leads to a qualitative understanding of the observed behaviour. The crossover behaviour of the critical exponents can be modeled and a quantitative analysis of the observed experimental data is presented.

I. INTRODUCTION

The influence of defects on the critical behaviour close to a structural phase transition has been studied both experimentally and theoretically for a long time. These investigations show that the critical behaviour can change dramatically compared to homogeneous systems. According to the Harris' criterium the critical behaviour is modified by quenched disorder if the critical exponent ν of the correlation length obeys the inequality $\nu > 2/d$ with d the spatial dimensionality of the system [1]. As a result the critical exponents near the phase transition temperature can change their values [2,3]. In addition a smearing out of the specific heat can be observed [4,5]. Furthermore the central peak, experimentally observed at $\omega = 0$ in the dynamical structure factor above the transition temperature, e. g. in $SrTiO_3$ [6,7], can be explained as a consequence of defects [4,8–10]. In recent years it has been found that the critical fluctuations above T_c reveal a second length scale in $SrTiO_3$ as well as in many others systems [11–13], a feature which has been reviewed by R. Cowley [14]. This phenomenon was observed in surface-near regions (typically $\approx 100\,\mu$m) [15,16] and the origin of the second length scale is considered to be the existence of defects [17].
In the present paper, we concentrate on the bulk behaviour where no sharp component occurs, also the central peak is not subject of our investigations, the behaviour of the sharp component will be discussed in a forthcoming paper (paper II) [18]. We have probed the cubic-to-tetragonal phase transition in $SrTiO_3$ at $T_c \approx 100\,$K with synchrotron radiation. The high **q**-space resolution and the high peak to background ratio obtained with triple-axis diffractometry at HASYLAB allows for detailed studies of the critical fluctuations at structural phase transitions [19,20].
The critical scattering above the antiferrodistortive transition of $SrTiO_3$ has been studied for samples with different oxygen vacancy concentrations. We measured the order parameter and the critical exponents of the correlation length and the susceptibility, the oxygen vacancy concentration in the samples was determined independently. The experimental findings from the scattering experiments are discussed quantitatively in terms of the influence of defects. In the theoretical discussion the static critical behaviour at structural phase transitions is considered with a Ginzburg-Landau functional, taking into account the influence of defects through a local increase of the critical temperature near the defects. The use of the replica trick makes it possible to investigate the static critical behaviour with the help of the renormalization-group theory [21,22]. However, in recent years a possible break down of the symmetry of the replica functional (replica-symmetry breaking RSB) is discussed [22–25]. Until now the influence of the free energy landscapes or "rare regions", which can occur for defect systems, has not been studied for structural phase transitions. Here the possibility of local order parameter clusters must be taken into account.

The paper is organized as follows: In Sec. II we present the experimental details and the results of the scattering experiments, followed by a description of the preparation and characterization of the samples. Sec. III provides the theoretical analysis of the experimental data, assuming first the qualitative behaviour and then the order parameter-states leading to the minimization of the free energy within the partition function. Finally, in Sec. IV we summarize and discuss our results.

II. EXPERIMENTAL RESULTS

The scattering experiments have been performed on 5 different samples using 120 and 100 keV synchrotron radiation at the undulator beamline PETRA II and the wiggler beamline BW5 at HASYLAB, respectively. All data have been collected at 3-axis-diffractometers in Laue geometry at the position of the (511)/2 superlattice reflection. In order to get both high incident photon flux and adequate **q**-space resolution in the scattering plane, annealed Si (311) crystals have been used as monochromator and analyzer. The resulting resolution (HWHM) in the scattering plane at BW5 (PETRA II) was $\Delta q_x = 1.5$–3×10^{-3}Å^{-1} ($\Delta q_x = 1\times10^{-3}$Å^{-1}) in the longitudinal direction and 2×10^{-4}Å$^{-1} \leq \Delta q_y \leq 2\times10^{-3}$Å^{-1} in the transverse direction, depending on the mosaicity of the respective sample. Perpendicular to the scattering plane the resolution was of the order of $\Delta q_z = 1\times10^{-1}$Å^{-1}. The experimental setup is described in detail in Refs. [26,16]. The deconvolution of the experimental data was performed as described by Hirota et al. [27].
In order to study the effect of oxygen doping, bulk measurements have been performed on a reduced, an oxidized and an as grown Verneuil single crystal. Additionally, a flux-grown sample [28] and an almost perfect crystal, grown by means of the float-zone technique [29], have been investigated. In Table I the different sample treatments and growth techniques are summarized. The behaviour of the sharp component in these samples will be discussed in paper II [18], in the following we only concentrate on the bulk properties.
The mosaicity of the Verneuil-grown crystals varied between 30" and 100" which is rather broad compared to the almost perfect float-zone grown (1"-7") and flux-grown samples (10"). However, the latter two crystals are slightly brownish, perhaps due to iron impurities [30], in contrast to the transparent as-grown Verneuil samples. Impedance measurements have been performed in order to determine the oxygen vacancy concentrations in the different samples [31]. Interestingly, the amount of oxygen vacancies is about two orders of magnitude bigger for the crystallographic

more perfect samples compared to the as grown and oxidized Verneuil-grown crystals. However, the reduced sample shows significant changes: the colour changes from transparent to black and the resistance decreases substantially, i. e. the amount of oxygen defects increases about three orders of magnitude. Impedance measurements with microelectrodes of different diameters [32,33] revealed a spatially homogeneous conductivity in the samples I and II. Owing to the relation between conductivity and oxygen vacancy concentration [31] it can be concluded that the concentration of the oxygen vacancies is distributed homogeneously over the respective samples. Assuming a random distribution of these vacancies the mean distance of defects results to $d = n^{-1/3}$ with n the defect concentration. This distance varies between $\approx 240\,\text{Å}$ for the lower defect concentrations and $\approx 40\,\text{Å}$ for the higher concentrations [see Table II].
In Fig. 1 the integrated intensity of the superstructure reflection (511)/2, normalized to the extrapolated value at $T = 0\,\text{K}$, is plotted versus the reduced temperature $\tau = \frac{T}{T_c} - 1$ for the different Verneuil-grown samples and the float-zone grown sample. Below T_c the intensity is following a power law with the critical exponent $2\beta = 0.68$, which is well known for $SrTiO_3$ [34,6]. Above T_c we observe a tail which is dependent on the defect concentrations. The tail above the critical temperature can originate from both the critical fluctuations and an additional contribution to the squared order parameter caused by defects. This can be interpreted in the way that static order parameter clusters exist at temperatures higher than T_c. Nevertheless, for the determination of the critical temperatures we followed the procedure explained in [6], i.e. at $T_c - \Delta T$ half of the intensity at $T_c + \Delta T$ has been substracted from the data of the integrated intensities of the superstructure reflections, which corrects for the effect of the critical scattering contribution to the integrated reflecting power of the superlattice reflection. The values of the critical temperatures, which have been found for the different samples, are given in Table II. A shift of the critical temperature to lower values with raising defect concentration is visible, which has been observed earlier in Refs. [35,36].
The inverse correlation length $\kappa_L(T)$ and the susceptibility $\chi_L(T)$ are deduced from the critical scattering at the (511)/2 superlattice reflection after deconvolution with the experimental resolution function. The critical scattering in the float-zone grown sample has been measured over a much larger temperature interval than those of the other samples. Here, a crossover between different values for the critical exponents ν and γ obtained from $\kappa_L(T)$ and $\chi_L(T)$ can be identified [see Fig. 2]. These data have been taken in the bulk of the float-zone grown sample but the probed volume also included two surfaces (the front and the back side). However, due to the relatively large thickness (12 mm) of the sample, the contribution of the sharp component to the signal, originating from a thin layer at the surface, was less than 1% close to T_c and has been neglected.
Around $\tau_c = 0.11$ a change of slope is clearly visible for both $\kappa_L(T)$ and $\chi_L(T)$. This crossover temperature τ_c is in excellent agreement with the value of τ_d [see Table II], which is defined as following: τ_d is the reduced temperature at which the correlation length $\kappa_L^{-1}(\tau_d)$ is equal to the mean distance d of the oxygen vacancies. Above this crossover temperature the system can be described within mean-field theory, which leads to exponents $\nu = 0.5$ and $\gamma = 1.0$, but below the crossover temperature the fitted exponents $\nu = 1.19(4)$ and $\gamma = 2.89(4)$ are much higher than theoretical values. The non-classical exponents expected for this 3d-Heisenberg system with cubic symmetry, calculated by LeGuillou et al. [37], are $\nu = 0.705(3)$ and $\gamma = 1.386(4)$.
In Figure 3 the inverse correlation length for the four other samples is plotted against the reduced temperature. Effective exponents ν and γ have been derived by fits of power laws to each data set without taking into account the crossover scenario, because the expected crossover temperature τ_d is either too small (≈ 0.02) or too large (0.20) to allow an observation of the crossover within the experimental probed temperature range. The effective exponents vary between $\nu \approx 0.7$, $\gamma \approx 1.4$ (as grown and oxidized Verneuil-grown samples) and $\nu \approx 1.2$, $\gamma \approx 2.4$ (reduced Verneuil-grown sample). It should be emphasized that the scaling relation $\gamma = (2 - \eta)\nu$, with $\eta \approx 0.03$ [38], still holds! Also, the scaling relation $2\beta = d\nu - \gamma$, which yields $\beta = 0.34(6)$ for the float-zone grown sample, is in excellent agreement with the experimental data below T_c.
In the following discussion an attempt is made to understand the microscopic nature of these experimental results.

III. THEORETICAL DISCUSSION

In our experimental measurements we found a smearing-out of the squared order parameter near the phase transition, which can be explained theoretically by the presence of local order parameter clusters above T_c [4,39,10]. Defects, which locally increase the transition temperature, lead to order parameter clusters above the critical temperature of the homogeneous system. For $SrTiO_3$ we expect a rotation of the oxygen octahedra near the position of oxygen vacancies to be responsible for finite order parameter clusters above T_c [40]. These rotations can occur around one of the three principal directions. Thus a three dimensional Heisenberg model should be used to model the critical behaviour. In Fig. 1 the solid line shows the fit to the experimental data using the power law for the normalized integrated intensity versus the reduced temperature $I^{1/2} \propto \tau^{0.34}$. Because $I^{1/2}$ is proportional to the order parameter, the value for the critical exponent β is in good agreement with the values obtained for the three dimensional

Heisenberg model in the homogeneous case [37]. But, in clear difference to the critical behaviour of homogeneous systems is the fact that for higher concentrations of oxygen vacancies a more pronounced tail exists [see Fig. 1 and Table II]. Of course the critical fluctuations also contribute to the strength of these tails. However, the contribution of the existing order parameter clusters and the dependence of the defect concentration is obvious. Unfortunately, for the experimental data investigated here, these two contributions cannot be differentiated adequately. Nevertheless, we clearly identified the first clear effect of defects on the critical behaviour. In an additional remark, we want to stress that our observation of a finite value of the squared order parameter does not mean that there exists a finite bulk value for the order parameter above T_c. The local order parameter clusters can be oriented in different directions in the order parameter space. If all clusters are oriented in one direction, a finite bulk value for the order parameter would result [see Ref. [10]].

For the float-zone grown crystal a crossover of the critical exponents ν and γ can be clearly observed as another effect of the defects [see previous Section], taking place at $\tau \approx 0.11$ [see Fig. 2]. This is the temperature range where the squared order parameter starts to be noticeable different from zero [see Fig. 1]. In the general picture of the influence of defects on the critical behaviour these findings can be understood as follows. Far away from the critical region mean-field exponents are expected, because fluctuations are small [41,42]. These mean-field exponents are found indeed for the float-zone grown crystal for $\tau > 0.11$ [see Fig. 2]. Lowering the temperature ($\tau \leq 0.11$) one has to take into account fluctuations and a crossover to non classical critical exponents should occur. Without defects, one would expect the critical exponents for the 3D Heisenberg model (e. g. $\nu \approx 0.705$ [37]). We find near the critical temperature for the float-zone grown crystal the value of the exponent $\nu = 1.19$ [see Fig. 2], which differs substantially from the one stated above. Because the correlation length becomes larger near the critical temperature, the critical fluctuations can become correlated over distances larger than the mean distance between the defects. In this case the impurities can change the critical behaviour and a crossover to a different critical exponent is possible. The Harris criterium defines the necessary condition [1]. If this condition is fulfilled, a dependence of the crossover temperature from the defect concentration should be observable. For the crystals probed here, with their different defect concentrations, we, indeed, find such a dependence [see Figs. 2,3 and Table II]. As described above the float-zone grown crystal has a crossover temperature equal to $\tau_d = 0.11$. For all other samples, except the reduced crystal, the characteristic temperature τ_d is very small (≤ 0.023) and thus the crossover itself is not visible in the experimental data. However, the critical exponents, obtained from power law fits to the data-sets in Figure 3, are smaller than $\nu = 1.19$ but larger than the Heisenberg-value 0.705. The crossover from the Gaussian exponents (e. g. $\nu = 0.5$) at high temperatures to the "defect-induced" exponents (e. g. $\nu \approx 1.2$) close to the critical temperature should lead to effective exponents ν_{eff} with values in the range $0.5 < \nu_{eff} < 1.2$, as observed.

For the strongly reduced sample the crossover takes place at very high temperatures ($\tau > 0.2$) so that the exponent $\nu = 1.2$, similar to the value observed in the float-zone grown crystal, is found in the whole temperature range probed here.

This again is in good agreement with the assumption that localized defects are responsible for the change in the critical behaviour. In the regime near the critical temperature T_c a critical behaviour different from the homogenous case, i. e. other critical exponents, should be observable. The critical exponents for systems with quenched disorder have been calculated before [1–3]. Those values can be compared with the critical exponents found in our experiments (e.g. in an ε-expansion for a 3-component order parameter $\nu = 0.5 + \varepsilon \cdot 9/64 + ... \approx 0.64$ with $\varepsilon = 4 - D = 1$ in three dimensions [3]). Unfortunately, we find in our experiments much higher values for ν and γ. One important question arises immediately: can we understand these findings within the concept of universality or are we facing non-universal behaviour? A first hint is that we find the scaling relation $\gamma = (2 - \eta)\nu$ still valid for all values of the critical exponents for the different crystals near the critical temperature [see Figs. 2,3]. As already discussed in the last section, the scaling relation for β holds, too.

In order to fully understand the experimental data in terms of the influence of defects on the critical behaviour the high values for the critical exponents ν and γ near T_c need to be explained. In the next two subsections we try to provide a theory which can explain the observed values for the exponents and can model the crossover behaviour.

A. Defect-functional

To investigate the questions arising from our experimental findings, the influence of local order parameter clusters, occuring above the critical temperature T_c, on the critical behaviour is taken into account. At low defect concentrations the order parameter clusters are supposed to be well isolated. Therefore, in the mean-field picture multiple local minima solutions exist, because the localized clusters can have different orientations in order parameter space [39]. The properties of such ground states were discussed for spin-glasses [22], random-ferromagnets [23], and recently for quantum magnets [24]. For random-ferromagnets Dotsenko et al. [23,43] found that the exponents calculated with the

help of the replica-method are unstable with respect to a possible breaking of the replica symmetry. New exponents result, different from those obtained by the usual replica-method. Even scenarios for possible instabilities of the theory are given. From these studies it is obvious that the states of minimal free energy in the partition function have to be considered in detail. In the present paper we sketch the theoretical derivation, for a more detailed discussion see e.g. [23,43,44].

The starting point for the theoretical discussion is a Ginzburg-Landau model for continuous structural phase transitions in disordered systems with quenched impurities. Until recently, in the standard approach only fluctuations around the homogeneous ground state of the order parameter $\varphi(x) = 0$ were considered in the replica-method [23]. We will incorporate fluctuations around the states with the lowest free energy in the partition function. The defect-functional used for the investigation of the effects of impurities on the free energy [10] reads

$$\mathcal{F}[\varphi(\mathbf{x}); U] = \int d^d x \left[\frac{1}{2} \sum_{i=1}^{k} \left((a + U)(\varphi^i(\mathbf{x}))^2 + (\nabla \varphi^i(\mathbf{x}))^2 \right) + \frac{b}{4} [\sum_{i=1}^{k} (\varphi^i(\mathbf{x}))^2]^2 \right] \tag{1}$$

Here $i = 1 \dots k$ denotes the component of the order parameter field, $a = a'(T - T_c^0)$ is the harmonic coefficient and vanishes at the bulk transition temperature T_c^0 of the pure system. The coefficient b of the non-linear term has to be positive. With the short-range potentials

$$U = \sum_{i_{\mathrm{D}}=1}^{N_{\mathrm{D}}} U(\mathbf{x} - \mathbf{x}_{i_{\mathrm{D}}}) \ . \tag{2}$$

the effects of randomly distributed defects at the sites $\mathbf{x}_{i_{\mathrm{D}}}$ $(i = 1 \dots N_{\mathrm{D}})$ are described. They can be considered as point like defects.

Applying the replica-trick [22], the averaging over different defect-distributions can be carried out, only taking into account fluctuations around the homogeneous ground state $\varphi(\mathbf{x}) = 0$. The discussion of the resulting fixed-points and flow equations can be found in Refs. [3,45].

To study the additional effect of possible order parameter clusters we start with the saddle-point approximation

$$-\Delta\varphi(\mathbf{x}) + (a + \sum_{i_{\mathrm{D}}=1}^{N_{\mathrm{D}}} U(\mathbf{x} - \mathbf{x}_{i_{\mathrm{D}}}))\varphi(\mathbf{x}) + b\,\varphi(\mathbf{x})^3 = 0 \ , \tag{3}$$

which gives the minimum solutions of the free energy. To keep the discussion transparent we choose the number of order-parameter components equal to one ($k = 1$). As far as we consider defects which locally increase the transition temperature, local order parameter condensates exist above T_{c}, as demonstrated in earlier studies [39,10]. In Fig. 4 a typical order parameter configuration is sketched. Thus in the presence of localized order parameter clusters, a more complicated solution of the ground state is found. However, as long as the concentration of the defects and the order parameter clusters is small, the value of $\varphi(x)$ outside these regions decays exponentially. The tail of such localized order parameter-clusters can approximately be written as $\varphi^i_{lok;0}(\mathbf{x}) \propto \frac{1}{|\mathbf{x}-\mathbf{x}_{i_{\mathrm{D}}}|}\, \mathrm{e}^{-|\mathbf{x}-\mathbf{x}_{i_{\mathrm{D}}}|/\ell}$ [39,10]. Therefore, an approximation of the extremal solution is [23,24]

$$\Phi^{(p)}(\mathbf{x}; U) = \sum_{i=1}^{N_{\mathrm{D}}} \sigma_i^{(p)} \cdot \varphi^i_{lok;0}(\mathbf{x}) \ , \tag{4}$$

with $p = 1 \dots L = 2^N$ possible solutions because of the Ising symmetry in the order parameter space ($k = 1$) for a given defect distribution U and $\sigma_i^{(p)} = \pm 1$. No finite order parameter results for well isolated and non-interacting order parameter clusters [10]. The clusters are of course temperature dependent, but we neglect this dependence here, assuming that in the temperature range where their contribution is most important the cluster structure does not change that much. Now we can write the partition function Z in a way that we consider the global minimum solutions $\Phi^{(p)}$ and fluctuations $\varphi(x)$ around these solutions

$$Z[U] = \int D\varphi(\mathbf{x}) \sum_{p=1}^{L} \mathrm{e}^{-\mathcal{F}[\Phi^{(p)}[\mathbf{x};U] + \varphi(\mathbf{x});U]} = \int D\varphi(\mathbf{x}) \mathrm{e}^{-\mathcal{F}[\varphi;U]} \cdot \tilde{Z}[U] \ , \tag{5}$$

where the part of Z with the contributions from the saddle point solutions is written as

$$\tilde{Z}[U] = \sum_{p=1}^{L} \mathrm{e}^{-\mathcal{F}[\Phi^{(p)};U]} \cdot \mathrm{e}^{-\int d^dx [\frac{3\,b}{2} \left(\Phi^{(p)}[\mathbf{x};U]\right)^2 \varphi(\mathbf{x})^2 + b\,\Phi^{(p)}[\mathbf{x};U]\varphi(\mathbf{x})^3]} \ . \tag{6}$$

Z and $\tilde{Z}$ depend on the actual defect potential U, because the free energy $\mathcal{F}$ does. Thus, we are still investigating the effect of frozen disorder. Because the system with defects is no longer translationally invariant, the trace in the partition function can no longer be treated in the usual way. The replica-method will be used to deal with the problem.

An additional remark concerning the energy barriers should be made. In our approach the existence of large energy barriers between the various saddle-point configurations is assumed. Unlike in glasses these barriers are not infinite. But as already pointed out by Narayanan et al. [24] in the thermodynamical limit these barriers tend to infinity. As a consequence also the dynamics of the clusters should be very slow. This gives us the possibility to consider just the statics and to neglect effects of relaxation and reorientation.

Performing the disorder average with the help of the replica trick by considering n replicas, the effect of order parameter clusters can be incorporated. With the saddle-point solution we find

$$Z_n = \langle \int D\varphi_1 \ldots D\varphi_n \ \mathrm{e}^{-\sum_{\alpha=1}^{n} \mathcal{F}[\varphi_\alpha;U]} \cdot \tilde{Z}_n[\varphi_1 \ldots \varphi_n;U] \rangle_U \ , \tag{7}$$

with the replica index α and

$$\tilde{Z}_n[\varphi_1 \ldots \varphi_n;U] = \sum_{p_1 \ldots p_n=1}^{L} \mathrm{e}^{-\sum_{\alpha=1}^{n} \mathcal{F}[\Phi^{(p_\alpha)};U]} \cdot \mathrm{e}^{-\int d^dx \sum_{\alpha=1}^{n} [\frac{3\,b}{2}\,\Phi^{(p_\alpha)}(\mathbf{x})^2 \varphi_\alpha(\mathbf{x})^2 + b\,\Phi^{(p_\alpha)}(\mathbf{x})\varphi_\alpha(\mathbf{x})^3]} \ . \tag{8}$$

This is the so called replica partition function for our problem. In the following the additional effect of order parameter clusters should be studied, thus the contribution of $\tilde{Z}_n[U]$ is our objective. The treatment of this kind of replica partition function was studied by Dotsenko et al. [23,43]. The authors analyzed the problems arising from this complicated structure for the solution of the partition function. As a result, they introduced two approximations to allow a treatment within the usual renormalization group theory, which will be discussed in the following.

Firstly, a distribution function for the local order parameter clusters $\varphi^i_{lok;0}(\mathbf{x})$ is presumed [23]. With that we interpret the solutions arising from the saddle-point approximation as random variables, even though for a given distribution of defects these solutions are fixed. However, we want to sum over all possible different distributions, hence this treatment is adequate. A Gaussian distribution function [23]

$$\begin{aligned} P[\{\varphi_{lok}(\mathbf{x})\}] \equiv P[\Phi^{(p)}(\mathbf{x};U)] &= \prod_{i=1}^{N_\mathrm{D}} \mathrm{e}^{-\frac{1}{2\Delta}\int d^dx [\varphi^i_{lok}(\mathbf{x})^2 - \varphi^i_{lok;0}(\mathbf{x})^2]^2} \\ &= \mathrm{e}^{-\frac{1}{2\Delta}\int d^dx [\Phi^{(p)}(\mathbf{x})^2 - \Phi_0(\mathbf{x})^2]^2} \ , \end{aligned} \tag{9}$$

with $\varphi^i_{lok}(\mathbf{x})$ as the local order parameter cluster is used. The parameter Δ depends on the distribution of the defect-strength, the temperature, and the coupling constant b. Furthermore, $\Phi_0(\mathbf{x})$ is the global solution $\Phi^{(p)}$ with $\varphi^i_{lok}(\mathbf{x}) = \varphi^i_{lok;0}(\mathbf{x})$. In this approximation Δ is treated as a constant parameter. The crucial point here is the assumption that $\Phi^{(p)}$ still is a solution of equation (7). Otherwise new interaction terms would be introduced in the functional.

Now the fluctuations have to be considered. For Δ small, $\Phi^{(p)}(\mathbf{x})^2 = \Phi_0(\mathbf{x})^2 + \delta\Phi^{(p)}(\mathbf{x})$, the fluctuations $\delta\Phi^{(p)}(\mathbf{x})$ around the saddle point solutions can be integrated out and it results [23]

$$\begin{aligned} \tilde{Z}_n \simeq \prod_{p=1}^{L} \left[\int D\,\delta\Phi^{(p)}(\mathbf{x}) \mathrm{e}^{-\frac{1}{2\Delta}\int d^dx \ \delta\Phi^{(p)}(\mathbf{x})^2} \right] \\ \times \sum_{p_1 \ldots p_n=1}^{L} \mathrm{e}^{\ \frac{b}{4}\int d^dx \sum_{\alpha=1}^{n} \delta\Phi^{(p_\alpha)}(\mathbf{x})^2 - \frac{b}{4}\int d^dx \sum_{\alpha=1}^{n} \delta\Phi^{(p_\alpha)}(\mathbf{x})[6\varphi_\alpha(\mathbf{x})^2 - 2\Phi_0(\mathbf{x})^2]} \ , \end{aligned} \tag{10}$$

defining $\Delta' = (1/\Delta - b/2)^{-1}$.

As a second approximation Dotsenko et al. suggested a heuristic ansatz to derive the leading contribution to the partition function $\tilde{Z}_n$ [23]. From the solution of the random-energy-models (REM) it is known that a partition function like $\tilde{Z}_n$ takes its maximum for $1 \leq x_0 \leq n$. For the REM it's possible to calculate the parameter x_0 by extremizing

the resulting free energy with respect to x_0. Unfortunately, in our problem the integration over fluctuations is done in a perturbative approach. This is why we cannot calculate the value of x_0 for the problem at hand explicitly. For a detailed discussion see Ref. [23].

Applying the two approximations stated above, a breaking of the symmetry of the replica-functional turns out to be significant for the Ginzburg-Landau-Wilson functional discussed here [23,44], which is a consequence of the fluctuations around the minimal free energy solutions $\pm\Phi_0(\mathbf{x})$. The form of the resulting functional was first derived by Dotsenko et al. [23]. Because the resulting form of the functional considered here is equivalent to the one discussed in Ref. [23], we want to refer for all the technical details to Ref. [23] and Ref. [43], especially for the derivation of the renormalization group flows and the calculation of the fixed points. To keep our discussion tight, we will focus on the interpretation of the results.

B. Crossover scenarios

After having shown how the breaking of the replica-symmetry can occur for the defect functional in Eq. (1), now the consequences for the critical exponents are discussed. To analyze the crossover effects we concentrate on the effective exponent ν_{eff} of the correlation length as a function of the reduced temperature τ.

From the renormalization group flow eqations, which are calculated to one-loop order [23], the Gaussian fixed-point and the Heisenberg fixed-point occur. They both prove to be unstable. But with the number of order parameter components k in $1 < k < 4$ a third, stable fixed point is possible. For example, the result for the critical exponent ν is

$$\nu = \frac{1}{2} + \varepsilon \, \frac{1}{2} \, \frac{3k(1-x_0)}{16(k-1) - kx_0(k+8)} \quad ; \tag{11}$$

with $x_0 = 0$ the usual replica symmetric value of the critical exponent ν is obtained [2]. Hence the effect of the breaking of the replica symmetry (where $x_0 \neq 0$) on the critical exponents can be interpreted as a reduction of the number of order-parameter components in a subtle manner.

As mentioned above, the value of x_0 cannot be derived in the approximation considered here. The experimental finding that asymptotically near T_c the values of the critical exponent ν are very similar, hints to the fact that there actually is only one x_0 for a particular class of defect systems. In Fig. 5 a set of possible flows of effective exponent ν_{eff} versus the reduced temperature is sketched. Depending on the initial values for the coupling constant b and the effective strength of the defects c [23,44], different crossover scenarios can result. Starting from the Gaussian fixed-point (large τ) the effective exponent ν_{eff} starts with its mean-field value. For smaller τ the Heisenberg fixed-point, calculated to one-loop order ($1/\nu_{eff} = 2 - \frac{k+2}{k+8}$), is reached, if the initial value for c is small. For larger initial values of the defect strength a direct crossover from the mean-field fixed-point to the "defect-induced" fixed-point is found. The width of the temperature where the crossover occurs, also varies with the initial values of c and b. Assuming $x_0 = 0.9622$, we can obtain the experimentally found critical exponent $\nu_{eff} = 1.19$ for $\tau \to 0$, that is in the critical regime. The temperature scale where the crossover takes place is dependend on the initial values of the coupling constants. By matching the temperature scale [46], the crossover can be modeled, too. For the float-zone grown sample the resulting fit of the experimental data is shown in Fig. 6.

Despite the remarkable agreement between theory and experimental findings one should be aware of the fact that this is only a one loop result. With a higher order in a loop expansion a similar fit might well require a different value for x_0. Through the two approximations, defined in the last subsection, a lot of physical effects which are very hard to model are condensed into the parameter x_0. The next goal of the theory should be to determine the value of x_0 and to answer the question if this parameter depends on the defect strength or the defect concentration. Dotsenko et al. expressed their hope that x_0 may be determined in higher order in ε, in which case universal exponents for a paticular class of defect sysems would result.

IV. DISCUSSION

In summary, we have investigated the effects of defects on the critical behaviour at structural phase transitions. Our experiments probed the $105\,K$ phase transition of $SrTiO_3$ and the influence of oxygen vacancies for different $SrTiO_3$ crystals.

We found in our experiments that the squared order parameter is non-vanishing and rounded above the critical temperature T_c, representing the transtion temperature for a perfect crystal. The rounded squared order parameter increases above this temperature with increasing concentration of oxygen vacancies in the crystals.

These effects were interpreted as a result of local order parameter clusters occuring above T_c (see Ref. [10]).

Furthermore, near T_c unusual high values for the critical exponents ν und γ were found in our experiments. For the float zone grown crystal we were also able to study a crossover of the critical exponents ν and γ in great detail. In addition, we identified a dependence of the crossover-temperature on the defect concentration of the respective samples.

The crossover scenario was analyzed in the framework of the renormalization-group theory (see also Refs. [47,46]). Two main effects could be studied here. Firstly, the correlation length of the critical fluctuations has to exceed the length scale of the mean distance between oxygen vacancies in order to change the values of the critical exponents of the homogeneous system. Secondly, the unusual high values for the critical exponents found experimentally below the crossover temperature, which indicate the crossover from classical to non-classical critical behaviour, could be explained by taking into account the fluctuations around the states of minimal free energy and the resulting breaking of the replica symmetry.

Because of the occurence of the paramter x_0 within the theory, which cannot be determined explicitly, some questions concerning the universal aspects of the results are still open. Two scenarios are possible: (i) the parameter x_0 is universal for certain classes of defect systems; (ii) the parameter x_0 depends on microscopic properties of the crystals and is not universal. We stated some hints that for the class of defect systems studied here universal behaviour occurs.

It is known from defect models [10] that in three dimensions there is a minimum strength of defects. Below this border no order parameter clusters form and the analyzed crossover should not occur.

It would be interesting to study similar systems in the presence of different kinds of defects or to study systems where the universality class can be changed, e.g. under pressure. Also further theoretical investigations are necessary to get a step beyond the approximations considered in this and in other papers that take into account the breaking of the replica-symmetry.

ACKNOWLEDGEMENTS

We would like to thank S. Rodewald and J. Fleig from MPI Stuttgart for the conductivity measurements, G. Shirane and H.J. Scheel for making available the float-zone and flux-grown $SrTiO_3$ crystals as well as S. Kapphan for preparing the Verneuil crystals, and U. C. Täuber and E. Courtens for fruitful discussion. Support from the DFG under contract number Schw12-1 is acknowledged.

[1] A. Harris, J. Phys. C **7**, 1671 (1974).
[2] D. Khmel'nitskiĭ, Sov. Phys.-JETP **41**, 981 (1975).
[3] G. Grinstein and A. Luther, Phys. Rev. B **13**, 1329 (1976).
[4] B. Halperin and C. Varma, Phys. Rev. B. **14**, 4030 (1976).
[5] B. Strukov, J. Taraskin, K. Minaeva, and V. Fedorikh, Ferroelectr. **25**, 399 (1980).
[6] T. Riste, E. Samuelsen, K. Otnes, and J. Feder, Solid State Commun. **9**, 1455 (1971).
[7] S. Shapiro, J. Axe, G. Shirane, and T. Riste, Phys. Rev. B **6**, 4332 (1972).
[8] D. Wagner *et al.*, Ferroelectrics **26**, 725 (1980).
[9] D. Wagner *et al.*, Z. Phys. B **37**, 317 (1980).
[10] F. Schwabl and U. Täuber, Phys. Rev. B **43**, 11112 (1991).
[11] S. Andrews, J.Phys.C **19**, 3721 (1986).
[12] T. Ryan, R. Nelmes, R. Cowley, and A. Gibaud, Phys. Rev. Lett. **56**, 2704 (1986).
[13] T. Thurston *et al.*, Phys. Rev. Lett. **70**, 3151 (1993).
[14] R. Cowley, Phys. Scr. T **66**, 24 (1996).
[15] H.-B. Neumann, U. Rütt, and J. Schneider, Phys. Rev. B **52**, 3981 (1995).
[16] U. Rütt *et al.*, Europhys. Lett. **39**, 395 (1997).
[17] S. Wang, Y. Zhu, and S. Shapiro, Phys. Rev. Lett. **80**, 2370 (1998).
[18] H. Hünnefeld *et al.*, Phys. Rev. B (2000), submitted.
[19] H.-B. Neumann *et al.*, J. Appl. Cryst. **27**, 1030 (1994).
[20] U. Rütt, H.-B. Neumann, H. Poulsen, and J. Schneider, J. Appl. Cryst. **28**, 729 (1995).
[21] S. Edwards and P. Anderson, J. Phys. F **5**, 965 (1975).
[22] M. Mézard, G. Parisi, and M. Virasoro, *"Spin Glass Theory and Beyond"* (World Scientific, Singapore, 1987).
[23] V. Dotsenko, A. Harris, D. Sherrington, and R. Stinchcombe, J. Phys. A: Math. Gen. **28**, 3093 (1995).
[24] R. Narayanan, T. Vojta, D. Belitz, and T. Kirkpatrick, Phys. Rev B **60**, 10150 (1999).
[25] E. Marinari *et al.*, J. Stat. Phys. **98**, 973 (2000).
[26] R. Bouchard *et al.*, J. Synchrotron Rad. **5**, 90 (1998).
[27] K. Hirota *et al.*, Phys. Rev. B. **52**, 13195 (1995).
[28] H. Scheel, J. Bednorz, and P. Dill, Ferroelctrics **13**, 507 (1976).
[29] G. Shirane and Y. Yamada, Phys. Rev. **177**, 858 (1969).
[30] C. Darlington and O. D.A., J. Phys. C **9**, 3561 (1976).
[31] I. Denk, W. Münch, and J. Maier, J. Am. Ceram. Soc. **78**, 3265 (1995).
[32] J. Fleig, F. Noll, and J. Maier, Ber. Bunsenges. Phys. Chem. **100**, 607 (1996).
[33] S. Rodewald, J. Fleig, and J. Maier, J. Europ. Ceram. Soc. **19**, 797 (1999).
[34] K. Müller and W. Berlinger, Phys. Rev. Lett. **26**, 13 (1971).
[35] J. Hastings, S. Shapiro, and B. Frazer, Phys. Rev. Lett. **40**, 237 (1978).
[36] D. Bäuerle and W. Rehwald, Sol.State Com. **27**, 1343 (1978).
[37] J. LeGuillou and J. Zinn-Justin, Phys. Rev. B **21**, 3976 (1980).
[38] M. Fisher, J. Math. Phys. **5**, 944 (1964).
[39] H. Schmidt and F. Schwabl, Z. Phys. B **30**, 197 (1978).
[40] M. Sato *et al.*, Phase Trans. **5**, 207 (1985).
[41] A. Levanyuk, Sov. Phys. JEPT **36**, 571 (1959).
[42] V. Ginzburg, Sov. Phys. Sol. State **2**, 1824 (1960).
[43] V. Dotsenko and D. Feldman, J. Phys. A: Math. Gen. **28**, 5183 (1995).
[44] B. Kaufmann, Ph.D. thesis, Technische Universität München, 2000.
[45] A. Korzhenevskii, K. Herrmanns, and W. Schirmacher, Phys. Rev. B. **53**, 14834 (1996).
[46] B. Kaufmann, F. Schwabl, and U. Täuber, Phys. Rev. B **59**, 11226 (1999).
[47] U. Täuber and F. Schwabl, Phys. Rev. B **46**, 3337 (1992).

Sample #	Growth technique	sample preparation	sample colour
I	**Floatzone grown**	-	Brownish, transp.
II	**Flux grown**	etched (89% H_3PO_4, 1h, 160°C)	Brownish, transp.
	Verneuil grown		
III	Oxidized	(48h, O_2-atm., 1bar, 1000°C)	Rose, transp.
IV	As grown	-	transparent
V	Reduced	(5h, H_2-atm., 1bar, 1250°C)	Black

TABLE I. Specifications of the samples investigated. Specimens grown by three different techniques (bold type) were available.

	T_c	n [cm^{-3}]	d [Å]	$\frac{1}{d}$ [10^{-3}Å^{-1}]	τ_d
Floatzone grown	98.8(1)	$6.1(2)\times10^{18}$	55(1)	18.2(2)	~ 0.115
Flux grown	102.6(2)	$2.8(2)\times10^{18}$	71(2)	14.2(3)	~ 0.035
Verneuil grown					
Oxidized	105.7(1)	$7.4(2)\times10^{16}$	238(2)	4.2(1)	~ 0.014
As grown	105.8(1)	$7.6(2)\times10^{16}$	236(2)	4.2(1)	~ 0.025
Reduced	101.0(1)	$1.7(1)\times10^{19}$	39(1)	25.7(5)	~ 0.20

TABLE II. Critical temperatures T_c and defect concentrations n of the different samples. $d = n^{-1/3}$ is the mean distance of defects, τ_d is taken from the measurements of the inverse correlation length ($\kappa(\tau_d) = d^{-1}$).

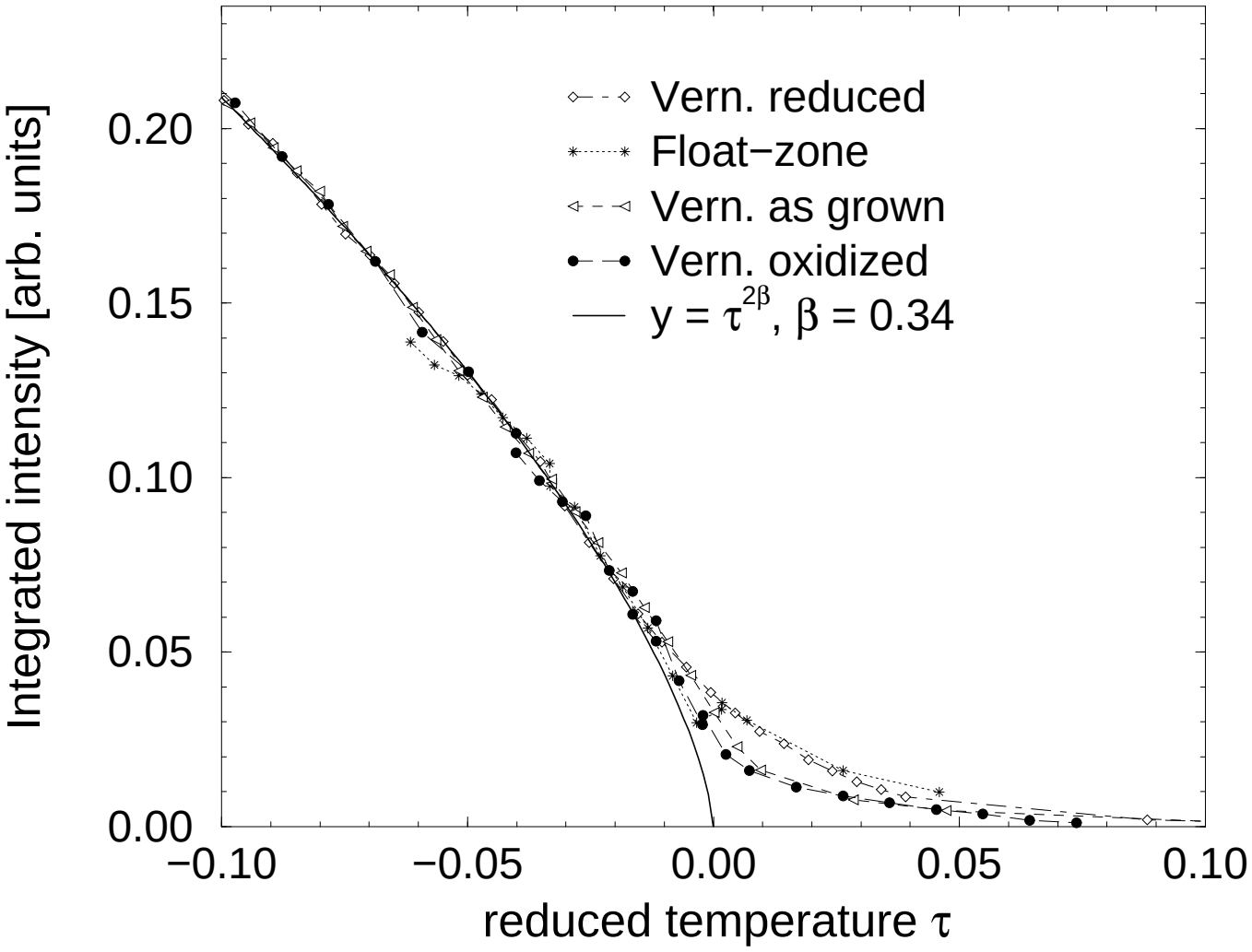

FIG. 1. Integrated intensities of the superlattice reflection (511)/2. In order to compare the tails above T_c the intensities have been normalized such that they coincide below the critical temperature. The critical exponent β has been fixed to $\beta = 0.34$.

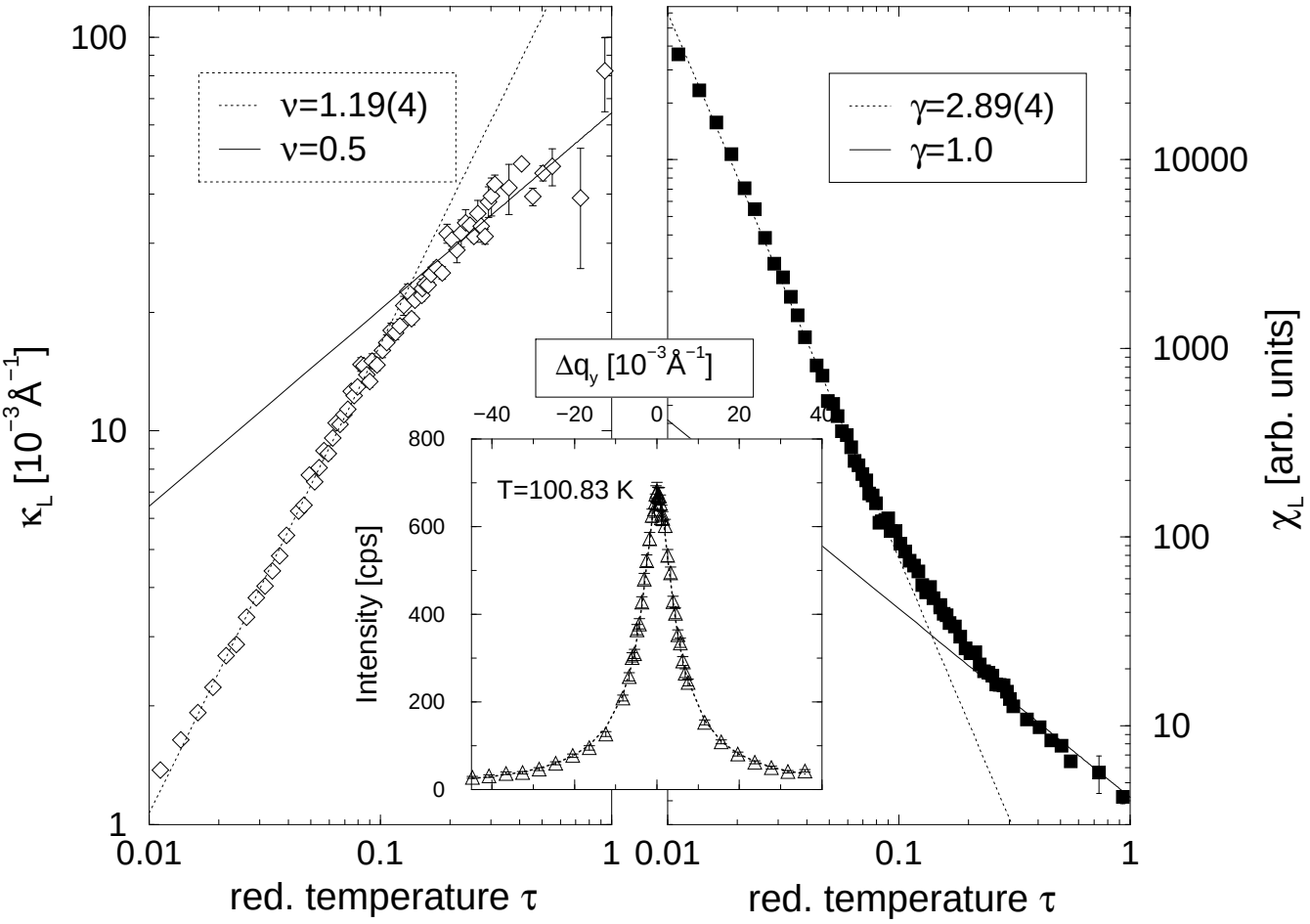

FIG. 2. Inverse correlation length and susceptibility of the broad component in the bulk of the Float-zone grown sample. Around $\tau_c = 0.11$ a crossover in the critical behaviour is clearly visible. The inset shows a transverse scan and the best fit to the data at $T = 100.8\,\mathrm{K}$.

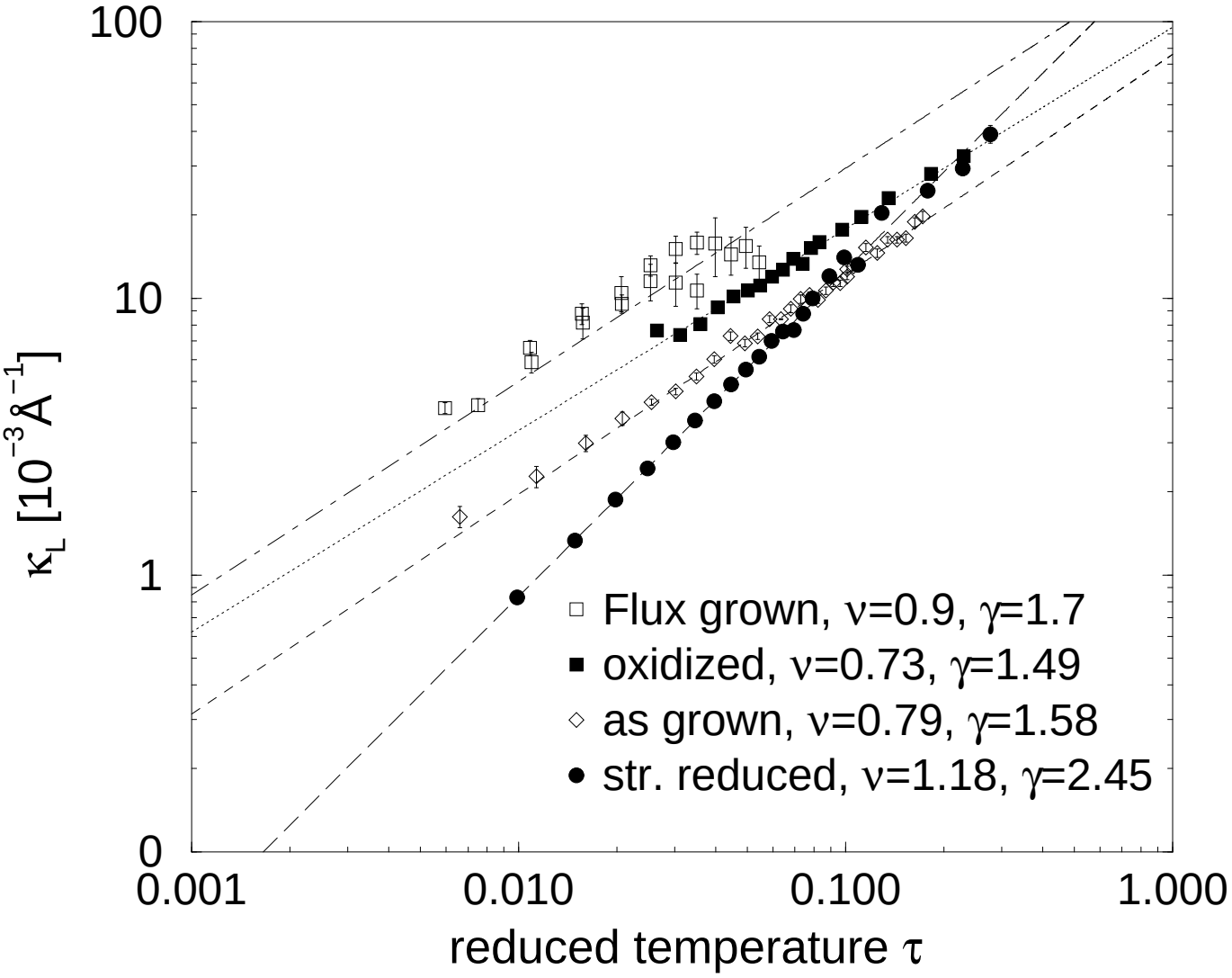

FIG. 3. Inverse correlation length for different samples. The effective exponents ν and γ have been derived from power law fits to the inverse correlation length and the susceptibility.

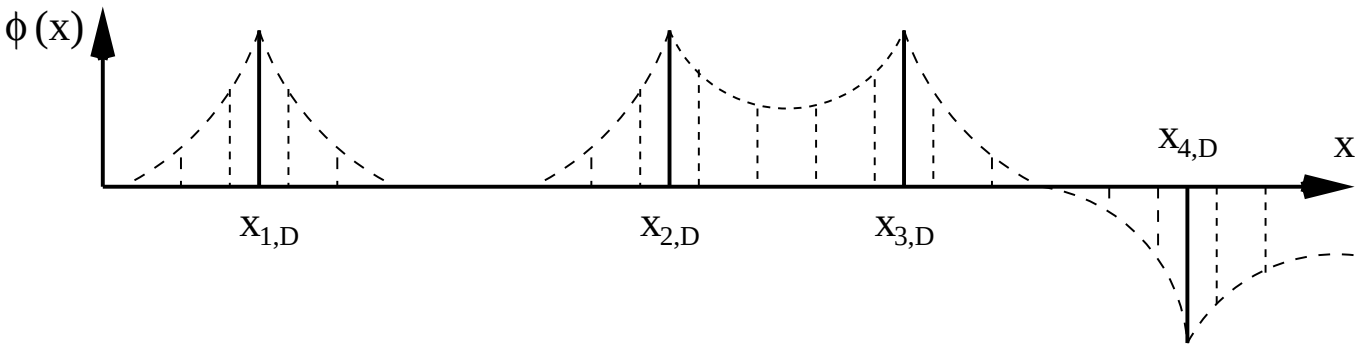

FIG. 4. A typical order parameter configuration above the critical temperature is sketched. Thus, in the presence of localized order parameter clusters a complicated solution of the ground state results.

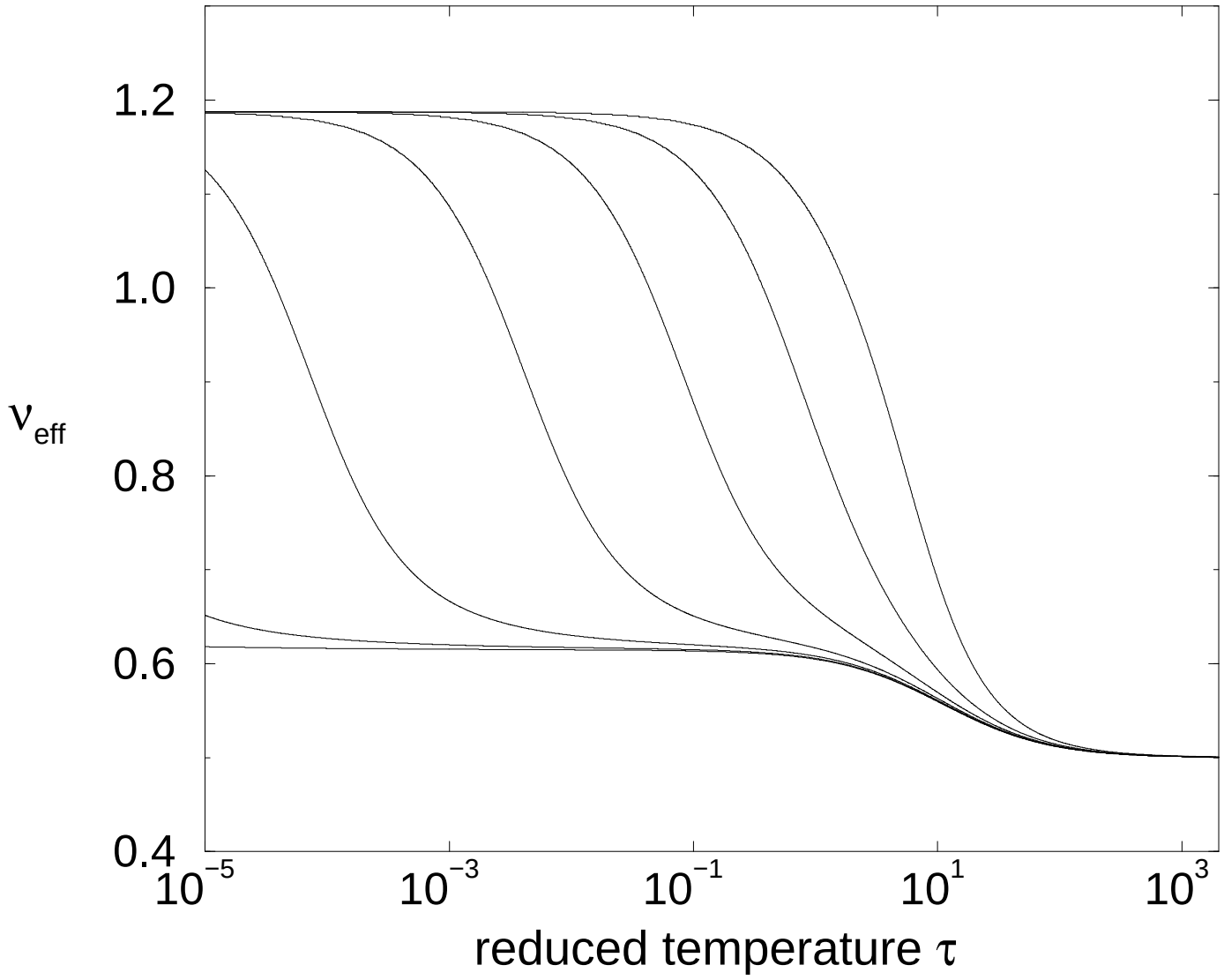

FIG. 5. The effective exponent ν is plotted against the temperature-scale for different initial values of the coupling constants. x_0 is choosen as 0.9622.

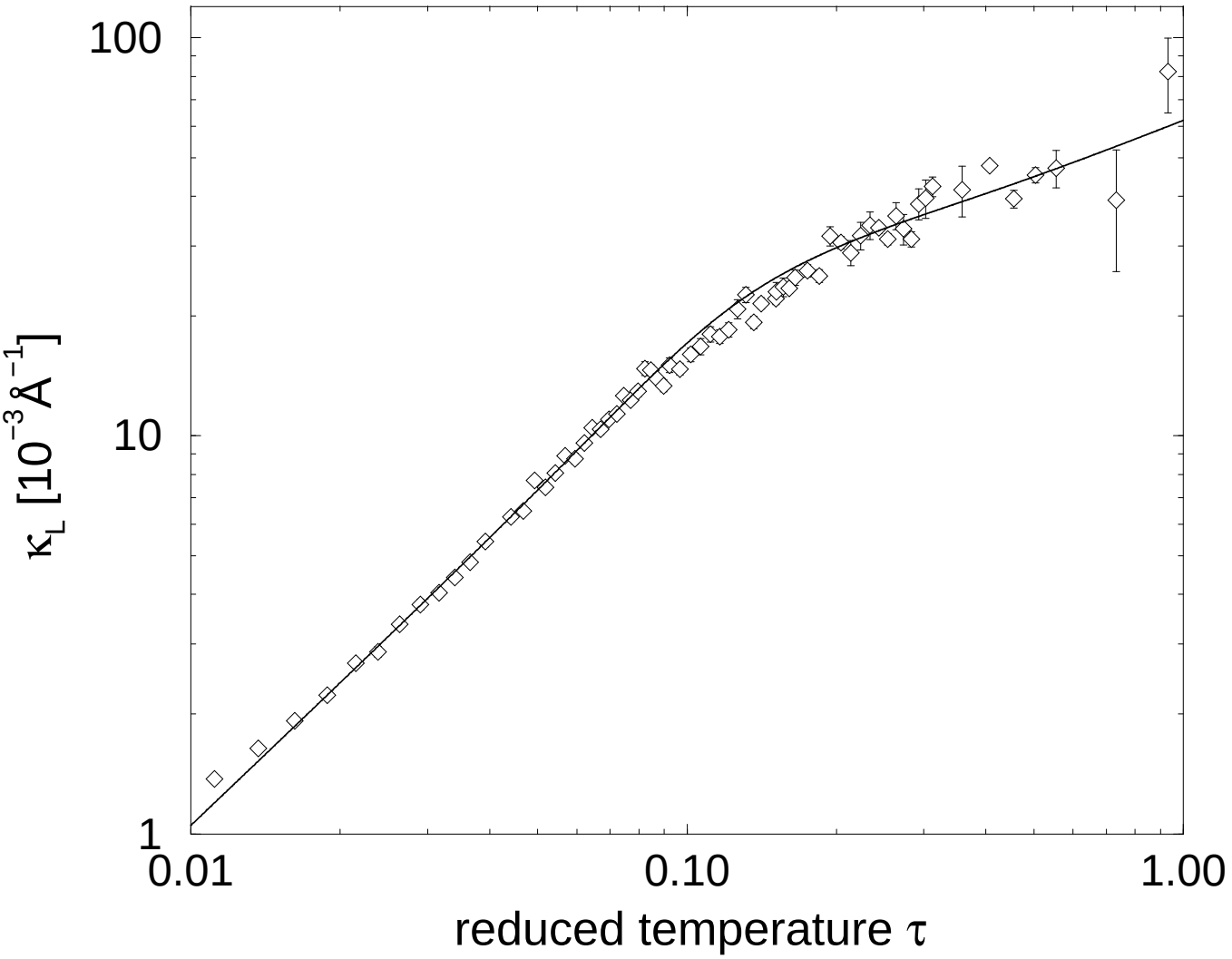

FIG. 6. Inverse correlation length of the broad component in the bulk of the float-zone grown sample. The theoretical curve models the crossover.